

Statics of Electromagnetic Bead Chains in Electromagnetic Field

*Nobuyuki Nakayama, Hiroyuki Kawamoto, Satoshi Yamada and Akiko Sasakawa
Department of Mechanical Engineering, Waseda University
Shinjuku, Tokyo, Japan*

Abstract

Experimental and numerical investigations have been carried out on statics of electromagnetic bead chains in an electromagnetic field. Chains formed on a solenoid coil were observed by a digital microscope and lengths and slant angles of chains were measured. Numerical calculations of chain forming process in the magnetic field were also conducted with the three-dimensional Distinct Element Method in consideration of the force due to magnetic interaction between particles. The chain forming process and the configuration of chains were simulated quantitatively. The axial bonding force of the chain in the electromagnetic field, which strongly relates to a bead-carry-out phenomenon in a magnetic brush development system, was also discussed.

Introduction

A schematic drawing of a magnetic brush development system¹ used for high-speed color laser printer is shown in Fig. 1. Magnetic carrier beads with electrostatically attached toner particles are introduced into the vicinity of a rotatory sleeve with a stationary magnetic roller inside it. Magnetized carrier beads in the magnetic field form chain clusters on the sleeve as shown in Fig. 2. Tips of chains touch the photoreceptor surface at the development area and toner particles on chains move to electrostatic latent images on the photoreceptor to form real images. Carrier chains play important roles in this development process in order to realize high quality imaging. It is necessary to clarify mechanical characteristics of formed chains and precise numerical calculation to simulate characteristics of chains is also indispensable for the improvement of the system.

In these points of view, statics of chains had been investigated in the previous study.² Lengths and slant angles of chains in the magnetic field were measured and calculated, and the mechanism of chain forming process was explained by the concept of energy minimization. It was also clarified that mechanical properties of chains can be simulated qualitatively by the two-dimensional Distinct Element Method (DEM).³ In this study, the numerical model is extended to three-dimensional and calculated results were compared to experimental ones. The axial

bonding force of the chain in the electromagnetic field was also evaluated.

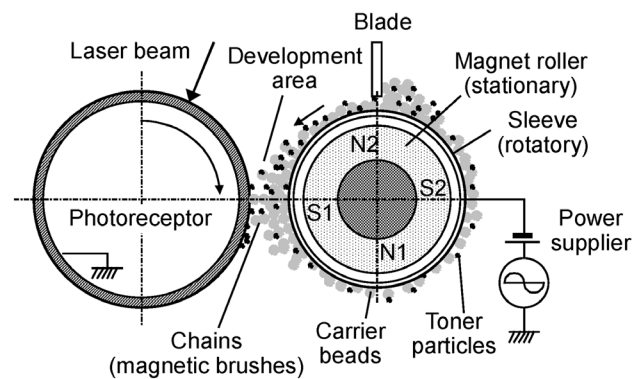


Figure 1. Magnetic brush development system in a laser printer.

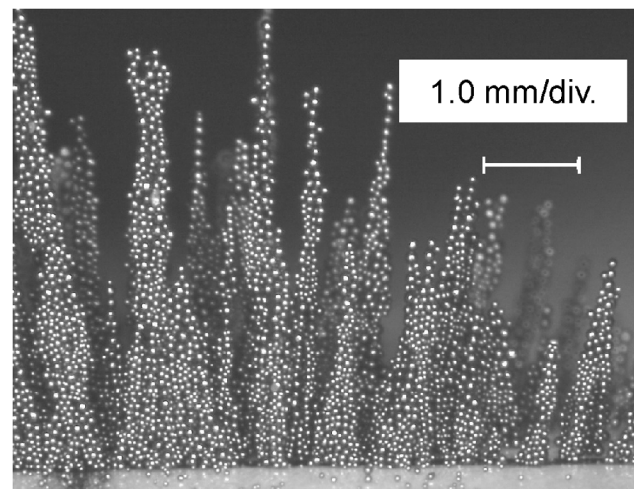


Figure 2. Chains of magnetic particles in magnetic field.

Experimental Method

Illustration and photograph of the experimental setup are shown in Fig. 3. Spherical, soft magnetic, and conductive particles (Toda Kogyo Corp.) shown in Fig. 4 were

provided in the area with 10 mm in diameter at the center of the end plate on a solenoid coil. Magnetic particles made by the polymerization method are 18-107 μm in diameter, 3500-3620 kg/m^3 in volume density, and 4.2-4.7 in relative magnetic permeability. Chains of magnetic particles formed in the magnetic field were observed and recorded by a digital microscope (Keyence Corp., VH-7000). Lengths and slant angles of chains were measured from stored still images.

Axial magnetic flux density B' along the center axis of the coil was measured and approximated by $B'(z) = B_0(1 - cz)$, where B_0 and c ($= 66.87 \text{ 1/m}$) are constants and z is the axial coordinate. ($z = 0$ at the surface of the end plate on which carrier beads were mounted.) B_0 is proportional to the coil current with a proportional constant 6.156 mT/A . This approximation was confirmed by theoretical and FEM calculations.

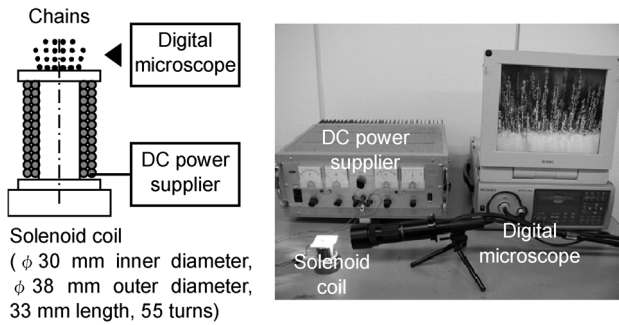


Figure 3. Experimental setup.

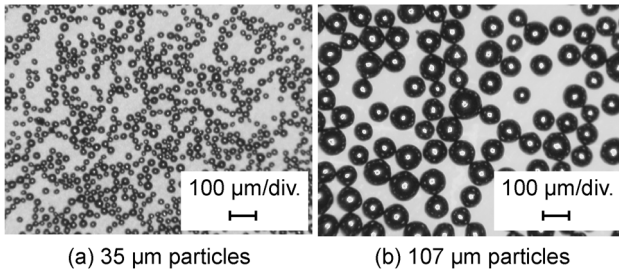


Figure 4. Photograph of magnetic particles.

Numerical Simulation

Numerical Method

Numerical simulation was performed on chain forming process based on the three-dimensional DEM. In the calculation, the following motion equation is solved for each particle with three degrees of freedom (u, v, w) excluding rotation.

$$m_j \ddot{\mathbf{u}}_j = \mathbf{F}_j, \quad (1)$$

where m_j , \mathbf{u}_j and \mathbf{F}_j are mass, displacement (u_j, v_j, w_j) and applied force of a j -th particle. In this study, mechanical interaction force, magnetic force, air drag, and gravitational force are included in the applied force, while van der Waals force and electrostatic force were neglected. The mechanical interaction force in the normal direction at the contact point was estimated from the Hertzian contact theory. The interaction force in the tangential direction was assumed to be proportional to the normal force with a proportional constant 0.25.

The magnetic force \mathbf{F}_{mj} of the j -th particle with the magnetic dipole moment \mathbf{p}_j are given by the following expression under the assumption that each particle behaves as a magnetic dipole placed at the center of the magnetized particle.

$$\mathbf{F}_{mj} = (\mathbf{p}_j \cdot \nabla) \mathbf{B}_j. \quad (2)$$

The magnetic flux density \mathbf{B}_j at the position of the j -th particle and magnetic moment \mathbf{p}_j are

$$\mathbf{B}_j = \mathbf{B}_j' + \sum_{\substack{k=1 \\ j \neq k}}^N \frac{\mu_0}{4\pi} \left(\frac{3(\mathbf{p}_k \cdot \mathbf{r}_{kj})}{|\mathbf{r}_{kj}|^5} \mathbf{r}_{kj} - \frac{\mathbf{p}_k}{|\mathbf{r}_{kj}|^3} \right) \quad (3)$$

$$\mathbf{p}_j = \frac{4\pi}{\mu_0} \frac{\mu - 1}{\mu + 2} \frac{a_j^3}{8} \mathbf{B}_j, \quad (4)$$

where N is the number of particles, μ_0 is the permeability of free space, μ is the relative permeability of particles, a_j is the diameter of the j -th particle and \mathbf{r}_{kj} is the position vector from the k -th to the j -th particle. The first term in the right hand side of Eq. (3) is the applied magnetic field by the coil and the second term is the field at the j -th particle due to dipoles of other particles. The magnetic force is determined by solving Eqs. (3) and (4) simultaneously and by substituting the results into Eq. (2).

In the simulation, a rectangular parallelepiped region is supposed as a calculation domain and particles with 88 μm in averaged diameter, 3550 kg/m^3 in volume density and 4.34 in permeability are placed uniformly in the domain. An example of the initial particle arrangement is shown in Fig. 5. In the case of Fig. 5, 3125 particles, which are equivalent to surface loading 0.64 kg/m^2 , are placed in the 2.5 mm square area. Each particle has a different radius that is normally distributed with 10% standard deviation. Young's modulus of the particles is assumed to be 10 GPa and that of the fixed boundaries is assumed to be 100 GPa. Poisson's ratio and the friction coefficient are assumed to be 0.3 and 0.2, respectively. At the first step of calculation, the motion of each particle is calculated every 100 ns in the gravitational field without magnetic field. Then the magnetic field equivalent to specific coil current is applied.

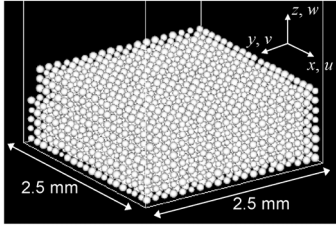


Figure 5. Initial arrangement of particles.

Numerical Results

Calculated chain forming process is shown in Fig. 6 compared with experimental observations. The magnetic field is equivalent to coil current 3 A and the maximum magnetic flux density is 18.5 mT. In the chain forming process, deposited particles disperse upward first due to the repulsive force between dipoles, then they form chain clusters to become magnetically stable state [0-20 ms]. The particles and clusters fall on the floor and grow up to treelike chains [20-40 ms]. Finally, stable corn shaped chains are formed by 40 ms. It is clearly recognized that the calculated chain forming process and the profiles are very similar to the experimental observations.

Time variation of potential energy in the chain forming process of Fig. 6 is plotted in Fig. 7. Although the gravitational energy increases with the dispersion of particles, magnetic and total potential energy decreases with time. The results strongly support the hypothesis that the stable chain configuration is determined to minimize its total potential energy which consists of gravitational and magnetic energy.²

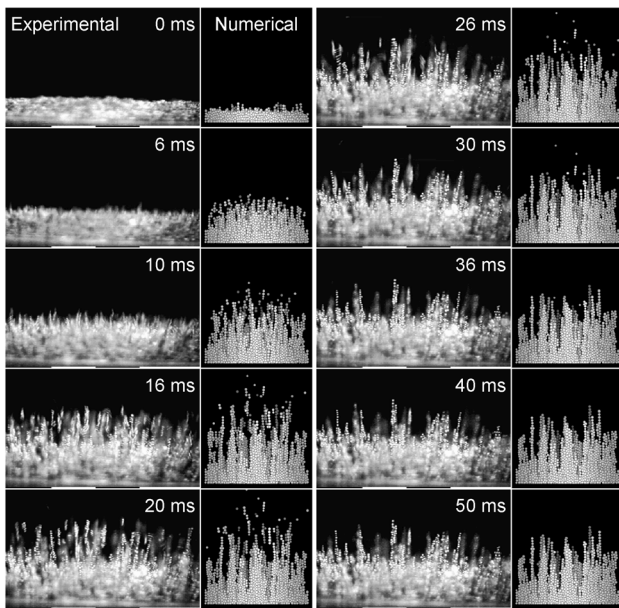


Figure 6. Time variation of chain profile. (averaged diameter 88 μm, surface loading 0.64 kg/m², coil current 3 A)

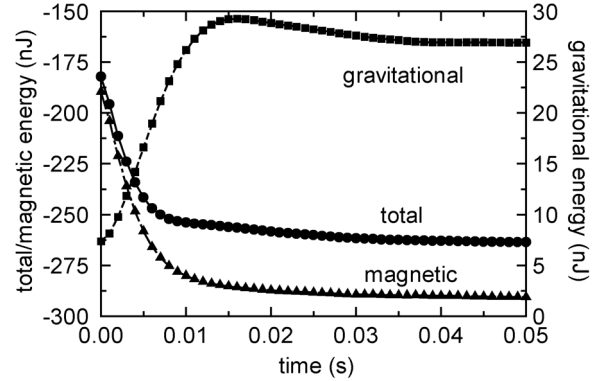


Figure 7. Time variation of potential energy.

Statics of Chains

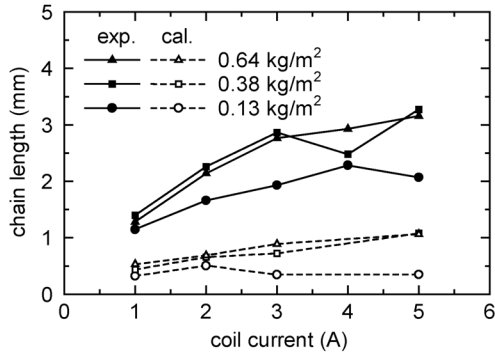
Length of Chains

Chain lengths are deduced from calculated chain profiles and results were compared to experimental ones. Calculated dependencies of maximum chain lengths on the coil current obtained by both two- and three-dimensional models are plotted in Figs. 8 (a) and (b), respectively. Measured chain length increases with the increase in the coil current and the surface loading of particles. It is shown that the two-dimensional results simulate the dependency qualitatively, however the quantitative accuracy is not sufficient. It is supposed to be the cause of disagreement in the two-dimensional calculation that the magnetic interaction force is not precisely evaluated. On the other hand, the three-dimensional results give fairly accurate results.

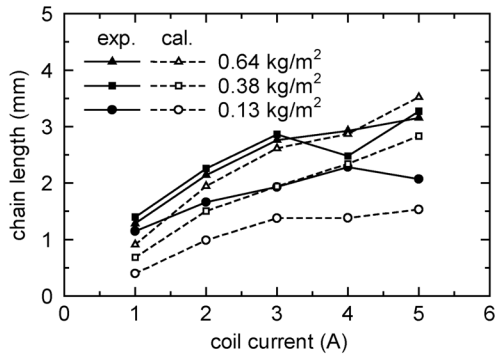
Inclination of Chains

Chains are inclined in the inclined magnetic field. Slant angles of chains were measured in the inclined magnetic field realized by inclining the coil to the gravity.⁵ It was already deduced in the previous investigation that the chain angle increased linearly with the increase in the inclination and the chain inclination exceeded that of the magnetic field by the gravitational force.² Additionally, if the inclination of the magnetic field exceeds a critical value, chains collapse.

These characteristics can be numerically simulated by applying inclined gravitational force to calculated chains. Examples of calculated inclination of chains are shown in Fig. 9. Figure 9 (a) shows a calculated chain profile at coil current 2 A and surface loading 0.64 kg/m² in normal gravitational field. Inclined gravity of angle θ_g was applied to the chains in (a), then chains incline as shown in (b) ($\theta_g = 40$ deg) and (c) ($\theta_g = 60$ deg). In the case of (c), some parts of chains are broken at the bottom of them and move to the boundary. The result corresponds to the collapse of chains observed in the experiment.

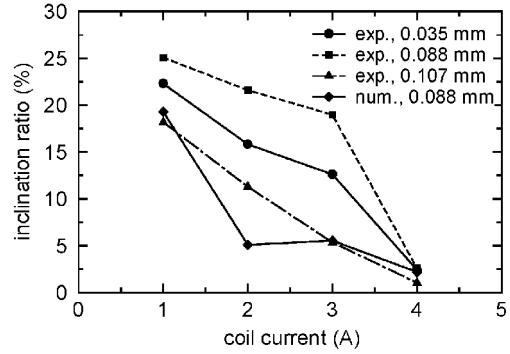


(a) Two-dimensional

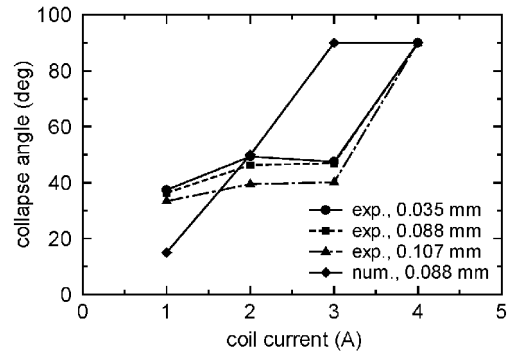


(b) Three-dimensional

Figure 8. Comparison of chain length obtained by numerical simulation with experimental results. (averaged diameter 88 μm)



(a) Inclination ratio



(b) Collapse angle

Figure 10. Comparison of calculated inclination ratio and collapse with experimental. (surface loading 0.64 kg/m^2)

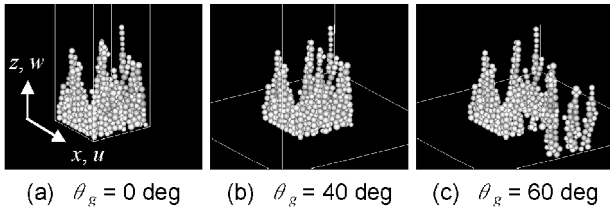


Figure 9. Calculated results of inclined chain.

Inclination ratios, defined as the ratios of excess angles of chain to the angle of the magnetic field, are plotted in Fig. 10 (a) and critical angles for the chain collapse are plotted in Fig. 10 (b). In Fig. 10 (b), experimental collapse angle is plotted as 90 degree for coil current 4 A, although the collapse were not observed in this case. It is clear that both the inclination ratio and critical collapse angle depend on the coil current. These results show that the lateral stiffness of chain increases with the increase in the magnetic flux density. Numerical results of inclination and collapse angle of chains plotted in Figs. 10 agreed qualitatively with the experimental.

Bonding Force of Chain

The behavior of chains under electromagnetic field was observed experimentally using similar setup as is shown in Fig. 3. Schematic diagram of the experimental setup is shown in Fig. 11. A pair of plate electrode was added on the coil, one was just on the end of the coil and another was separated by the gap 6.2 mm and parallel to the electrode on the coil. The voltage V was applied between the electrodes. If the sufficient electric field was applied to chains in the magnetic field, some chains broke and particles at the top of the chains move to the opposite electrode. These phenomena are well known as “bead-carry-out” in the magnetic brush development process. The critical electric field to break chains was measured in the experiment.

The experimental results are plotted in Fig. 12. The electric field was estimated by V/d , where d is a gap between the top of the chain and the upper plate electrode. Electric fields to move the first, the second, and the third particle are plotted in the figure. The electric field to break chains increased nonlinearly with the increase in coil current.

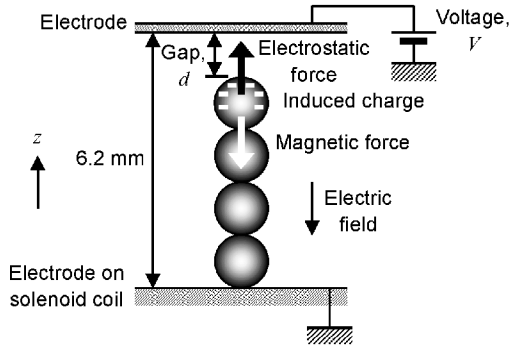


Figure 11. Schematic diagram of chain in electromagnetic field.

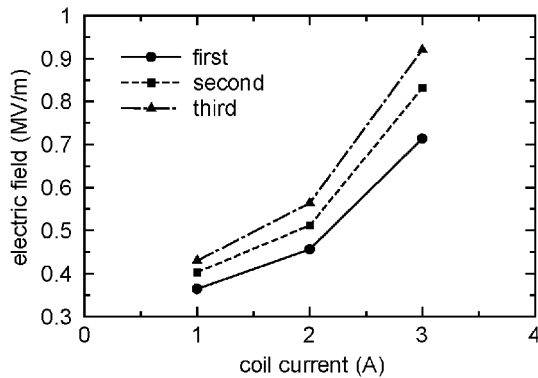


Figure 12. Critical electric field to break chains. (averaged diameter 88 μm , surface loading 0.64 kg/m^2 , coil current 3 A)

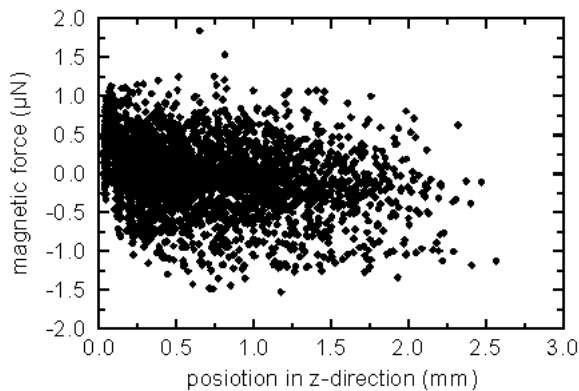


Figure 13. Distribution of magnetic force. (averaged diameter 88 μm , surface loading 0.64 kg/m^2 , coil current 3 A)

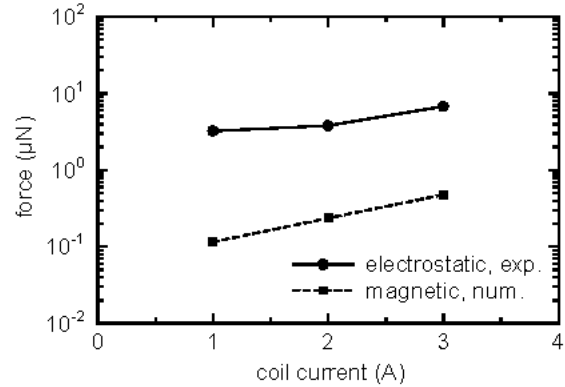


Figure 14. Electrostatic and magnetic force applied to the particle.

On the other hand, calculated magnetic bonding forces in z -direction are plotted in Fig. 13 for the case shown in Fig. 6 at 50 ms after applying magnetic field. The absolute value of the force is μN order.

Assuming a completely charged sphere-plate condenser with diameter a , voltage V and gap d , electric forces, F_e were estimated by Eq. (5) from the experimental results shown in Fig. 12.

$$F_e = \frac{\pi \epsilon_0 a (2d + a) V^2}{d^2}, \quad (5)$$

where ϵ_0 is the dielectric constant of free space. The results are shown in Fig. 14 comparing with the calculated magnetic bonding force. The calculated magnetic force in Fig. 14 is the average value of the highest 10 particles. As mentioned before, the electrostatic and magnetic force, that is the bonding force in the electrostatic measurement and the calculated magnetic bonding force, increase with the increase in coil current. However, there is a significant discrepancy between the measured and the calculated bonding force. Further studies on the numerical estimation of electromagnetic forces are being conducted.

Conclusion

Experimental and numerical investigations have been carried out on statics of electromagnetic bead chains in an electromagnetic field. Lengths and inclinations of chains formed on a solenoid coil were measured and numerically simulated by the three-dimensional DEM in consideration of magnetic interaction force between particles. The dependencies of chain length on both the surface loading of particles and the magnetic flux density, and those of the enlargement of chain inclination and critical collapse angle on the magnetic flux density can be simulated accurately with the three-dimensional DEM. Finally, the axial bonding force of chains in electromagnetic field was investigated. It was clarified that both the bonding force in the electrostatic measurement and the calculated magnetic bonding force become large in the high magnetic field.

Acknowledgement

The authors would like to express their thanks to Toda Kogyo Corp. for supplying magnetic particles, and to N. Sukou, S. Nakatsuhara and H. Takahashi (Waseda Univ.) for their help of carrying out experiments. This work is supported by Hosokawa Powder Technology Foundation.

References

1. E. M. Williams, *The Physics and Technology of Xerographic Processes*, Krieger Publishing, FL (1993).
2. N. Nakayama, H. Kawamoto and M. Yamaguchi, Statics of Magnetic Bead Chain in Magnetic Field, *J. Imaging Sci. Technol.* (to be published).
3. P. A. Cundall and O. D. L. Strack, A Discrete Numerical Model for Granular Assemblies, *Géotechnique*, **29**, 1 (1979), 47-65.

4. R. S. Paranjpe and H. G. Elrod, Stability of Chains of Permeable Spherical Beads in an Applied Magnetic Field, *J. Appl. Phys.*, **60**, 1 (1986), 418-422.
5. H. Kawamoto, N. Nakayama, S. Yamada and A. Sasakawa, Resonance Frequency and Stiffness of Magnetic Bead Chain in Magnetic Field, *IS&T's NIP18: 18th International Conf. On Digital Printing Technologies*, p. 28 (2002).

Biography

Nakayama, Nobuyuki holds a BS degree in Physics from Tohoku Univ. (1983). In 1983, he joined Fuji Xerox, and has been engaged in the research of electrophotography as a Researcher. From 2000, he has also been a student of Department of Mechanical Engineering, Waseda Univ. He is working on numerical simulation and measurement of powder dynamics in electrophotography. He is a member of the Imaging Society of Japan and the Japan Society of Mechanical Engineering.